# A High-Resolution, Four-Band SAR Testbed with Real-Time Image Formation

Bruce Walker, Grant Sander, Marty Thompson, Bryan Burns, Rick Fellerhoff, and Dale Dubbert
Sandia National Laboratories, P. O. Box 5800
Albuquerque, NM 87185-0529
(505) 844-1261; fax: (505) 844-0858; e-mail: bcwalke@sandia.gov



## ABSTRACT

This paper describes the Twin-Otter SAR Testbed developed at Sandia National Laboratories. This SAR is a flexible, adaptable testbed capable of operation on four frequency bands: Ka, Ku, X, and VHF/UHF bands. The SAR features real-time image formation at fine resolution in spotlight and stripmap modes. High-quality images are formed in real time using the overlapped subaperture (OSA) image-formation and phase gradient autofocus (PGA) algorithms.

## INTRODUCTION

In cooperation with numerous sponsors, Sandia National Laboratories has developed a multimode SAR testbed capable of operation on four bands: Ka band (32.6 - 37.0 GHz), Ku band (14 - 16 GHz), X band (7.5 - 10.2 GHz), and VHF/UHF (125 - 950 MHz). The SAR achieves state-of-the-art resolutions on each band while forming the SAR images in real time. Exceptional real-time image quality is achieve through the use of innovative image-formation and autofocus algorithms as well as high-accuracy motion measurement and compensation. A Twin-Otter aircraft (Figure 1) provides a flexible, low-cost platform for the SAR. The SAR testbed is designed to be very adaptable -- hundreds of parameters may be readily changed to meet the needs of new experiments.

Table 1 summarizes the parameters for the Twin-Otter SAR. The SAR operates over a wide range of resolutions, depression angles (2 to 90 degrees), squint angles (greater than ±45 degrees from broadside depending on operating parameters), and ranges (1 to 16 km). Both VV and HH polarizations are available on each frequency band, except Ka band which currently uses only VV. Cross polarization, HV, is available at the VHF/UHF band. In the spotlight mode, dwell times in excess of 60 seconds have been demonstrated with excellent image quality.

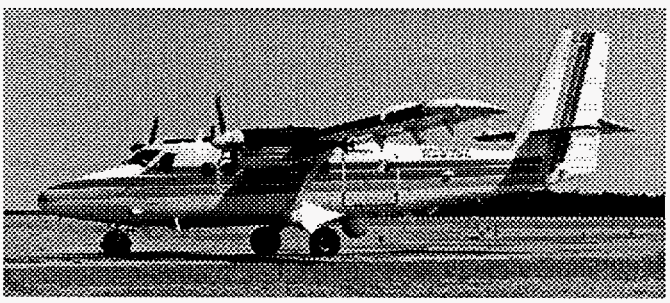

**Figure 1. Twin-Otter Aircraft**

**Table 1. Twin-Otter SAR Parameters**

| Parameter | Value | Units |
|---|---|---|
| Operating frequency | | |
| VHF/UHF | 125 to 950 | MHz |
| X band | 7.5 to 10.2 | GHz |
| Ku band | 14 to 16 | GHz |
| Ka band | 32.6 to 37.0 | GHz |
| Range | 1 to 16 | km |
| Aircraft velocity | 35 to 70 | m/s |
| Spotlight resolution | 1 to 3 | m |
| Stripmap resolution | | |
| VHF/UHF | 2 to 10 | m |
| X, Ku, and Ka bands | 1 to 3 | m |
| Swath width | 1792 | pixels |
| Depression angle | 2 to 90 | degrees |
| Squint angle | < 45 to > 135 | degrees |
| Noise equivalent reflection coefficient (band dependent) | < -30 | dB |
| Peak sidelobes | < -35 | dBc |
| Multiplicative noise ratio | < -10 | dB |
| Dynamic range | > 75 | dB |
| Absolute RCS calibration, 3σ | < ± 3 | dB |

## OPERATING MODES

The Twin-Otter SAR can operate in either of the conventional stripmap or spotlight SAR modes. Figure 2 is an example of the stripmap mode where four stripmap passes of the Washington, DC area have been mosaiced. In addition to stripmap and spotlight modes, the SAR is capable of flying circles around targets in a spotlight mode. Circular data collections provide a means of efficiently characterizing targets over a wide range of aspect angles.

Several enhancements have been added to the Twin-Otter SAR beyond the conventional SAR modes. At Ku-band, a two-antenna configuration provides 3-D or interferometric SAR (IFSAR) capability. Using careful calibration procedures, height accuracies of sub-meter rms are

This work was supported by the United States Department of Energy under Contract DE-AC04-94AL85000.

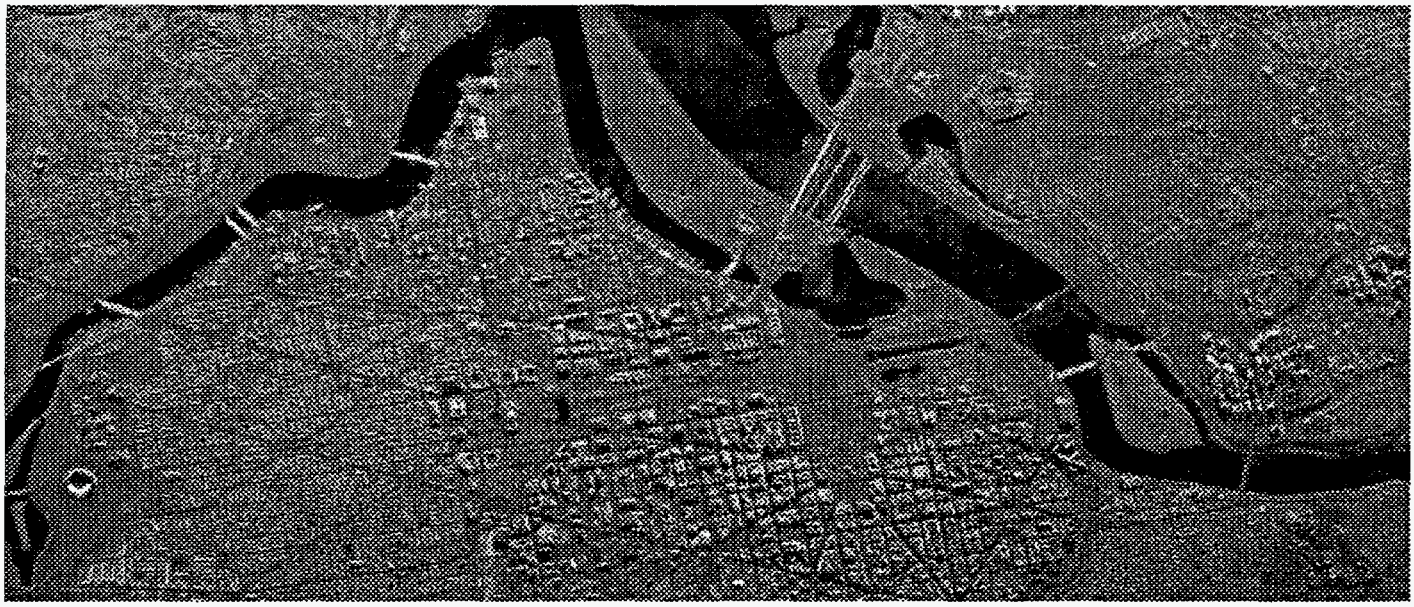

**Figure 2. SAR Image of Washington, DC at 1-m Resolution, Ku Band**

achieved. The IFSAR has been used to map rural as well as urban regions. A novel phase-unwrapping technique [1] uses an amplitude-monopulse measurement to aid in unwrapping the phase ambiguities. This technique provides unambiguous height measurements and greatly improved computational efficiency compared to estimation-based phase-unwrapping algorithms. Figure 3 shows an IFSAR image of a rural area near Albuquerque, NM, yielding height noise of about 0.5-m rms.

Additional enhancements include coherent change detection for detecting decorrelation or minute changes in radar scattering and a bistatic SAR mode which does not require direct-path synchronization between the transmitter and receiver. RF tags or transponders have been demonstrated which can be encoded within a SAR image.

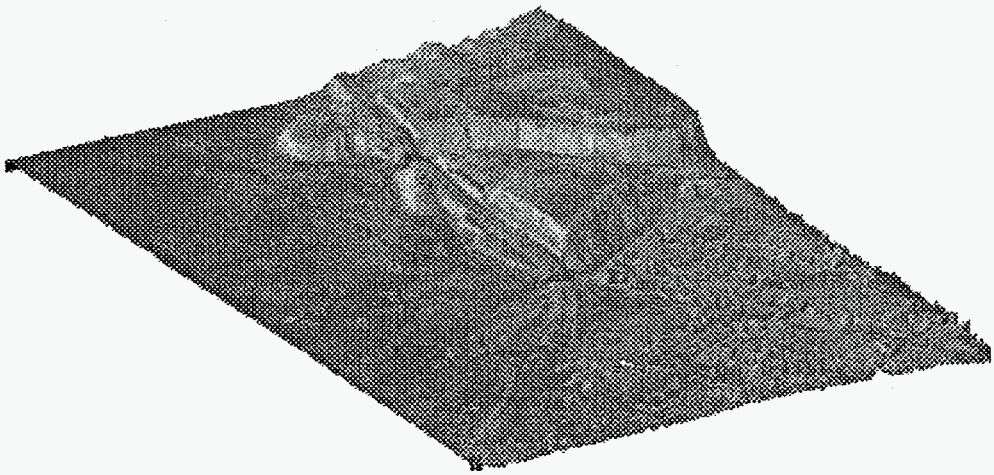

**Figure 3. Rendering of Interferometric SAR Image of Black Mesa, NM**

## HARDWARE DESCRIPTION

Figure 4 shows a simplified block diagram of the base Ku-band SAR. The antenna, inertial measurement unit (IMU), and rf front end are located on the gimbal as shown in Figure 5. Figure 6 shows the Radar Assembly which contains the digital-waveform synthesizer, frequency converter (exciter), two-channel receiver, A/D converter, and image-formation processor.

Four frequency bands are achieved by frequency translating to the desired frequency band from the base Ku-band SAR. The addition of an antenna, rf front end, transmitter, and frequency translator allow the Ku-band SAR to be readily adapted to different frequencies. This technique minimizes the new hardware required. To date, three additional frequency bands have been added: Ka, X, and VHF/UHF. The VHF/UHF band is actually designed to allow non-continuous coverage from 5 MHz to 2 GHz; however, the current antenna limits the low-end frequency at 125 MHz and the transmitter limits the high-end frequency at 950 MHz.

The Sandia SAR platform combines five primary technologies which are each essential to the formation of high-quality, fine-resolution images in real-time:

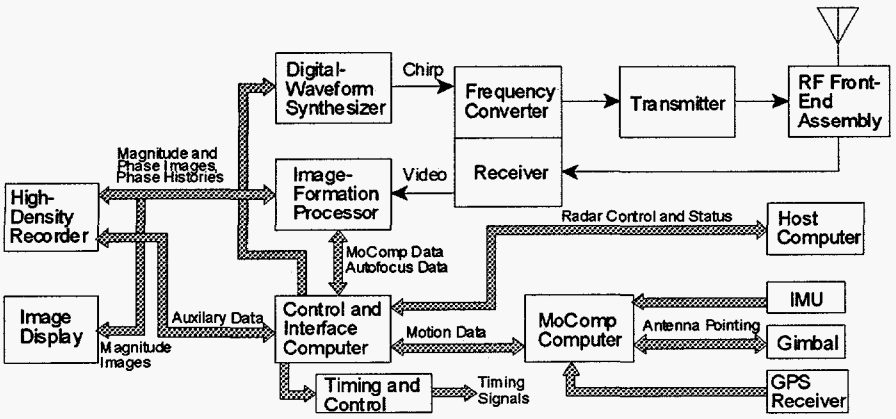


**Figure 4. Simplified Block Diagram of the Twin-Otter SAR**

- Digital-waveform synthesizer with RF phase-error correction,
- Linear-phase, wide-bandwidth microwave subsystems,
- Real-time image-formation processor which implements both the overlapped-subaperture (OSA) and phase-gradient autofocus (PGA) algorithms,
- High-accuracy motion measurement and precision GPS-aided navigation, and
- Real-time motion compensation of the transmitted waveform and received samples.

The digital-waveform synthesizer (DWS) generates a linear-FM or chirp waveform for both the transmit and receive LO (deramp) signals. The DWS consists of two digital-phase-generator GaAs ASICs, each driving a GaAs sine look-up-table read-only memory (ROM). Each phase-generator and sine-ROM pair operates at 400 MHz, both driving an input-multiplexed GaAs digital-to-analog converter (DAC) to yield the analog chirp output. The two circuits are synchronized and clocked at 800 MHz to yield a theoretical bandwidth of DC to 400 MHz for the chirp output.

The frequency converter, transmitter, and receiver subassemblies achieve phase-linearity across wide bandwidths through stringent phase-error allocations and novel phase-cancellation techniques. In addition to predistorting the transmitted waveform to compensate for phase nonlinearities, rf circuits have been developed which cancel the phase nonlinearities of other rf components. These technologies achieve excellent image quality, with azimuth and range sidelobes below -35 dBc.

The real-time image formation processor is a custom design based on the digital-array signal processor and programmable-array controller (DASP/PAC) FFT chipset from Signal Processing Technologies (SPT). Six DASP/PAC FFT boards provide the primary computational throughput required. Two TMS320C30 control computers provide the motion compensation, autofocus, and control functions.

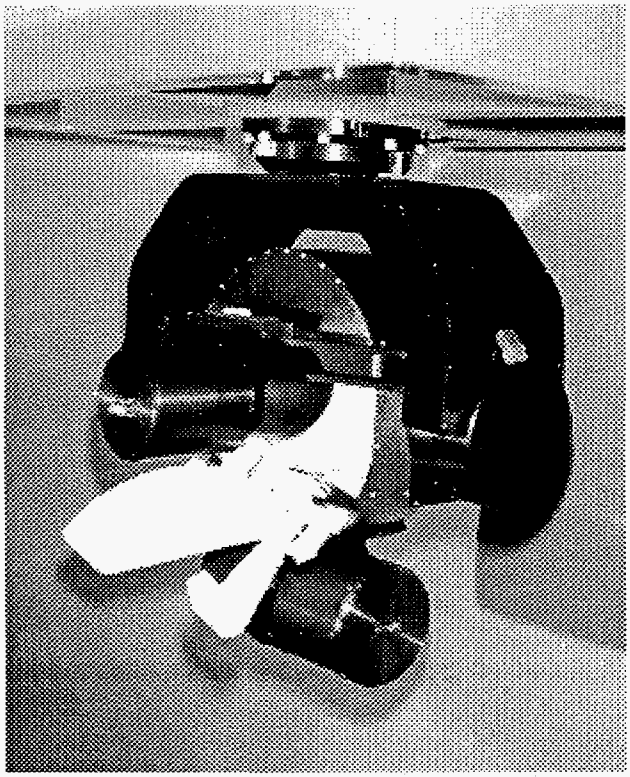

**Figure 5. Antenna Assembly**

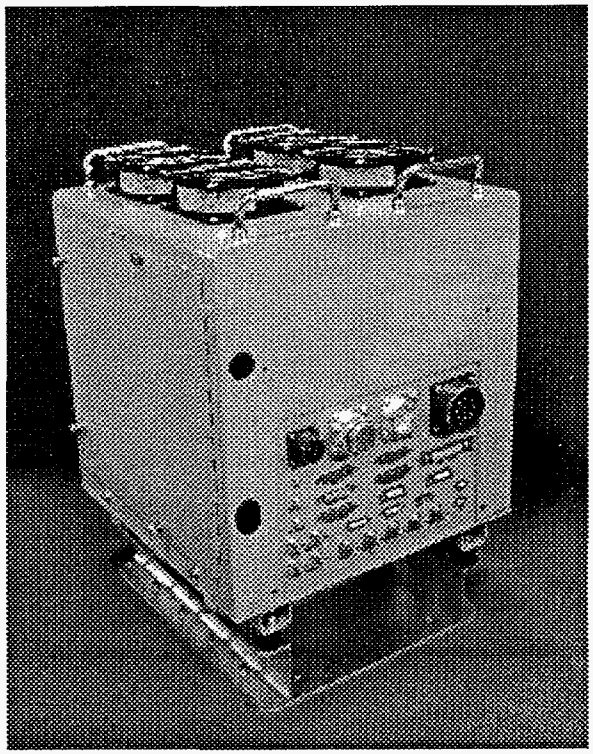

**Figure 6. Radar Assembly**

Three short 19-in racks contain the navigation operator interface, radar operator interface, image display, high-density tape recorders, and power supplies. Two commercial PCs provide the navigation and radar operator interfaces, allowing mission or radar operation changes to be easily made. The SAR image is displayed in real-time on a 2048 x 2560-pixel MegaScan monitor. An Ampex DCRSi recorder stores the radar phase history data, the complex image data, and other auxiliary data, such as motion measurement, state-of-health, etc. A Metrum VLDS recorder may also be used as a backup recorder in storing the image data.

## IMAGE-FORMATION ALGORITHMS

The image-formation processor implements the overlapped subaperture (OSA) image-formation and phase-gradient autofocus (PGA) algorithms in real time. The OSA algorithm [2] enables real-time image formation through innovations in digital-waveform synthesis, A/D sampling, and high-accuracy motion measurement. These technologies allow real-time motion compensation of the transmitted waveform and received samples, simplifying real-time image formation.

To form fine-resolution SAR images, an algorithm that can compensate for significant non-straight-line motion is required. The OSA algorithm was designed to be a real-time solution to this problem. The algorithm is constructed entirely with FFT and vector-multiplication operations. Some motion-compensation steps are carried out before the return signal is processed by changing the radar center frequency and phase, PRF, and A/D converter sample rate. The radar computes these parameters as functions of motion data provided by the motion-measurement system.

Figure 7 is a simplified functional diagram of the OSA algorithm. The algorithm is composed of three basic steps: coarse-resolution azimuth processing, fine-resolution range processing, and fine-resolution azimuth processing. In OSA, a synthetic aperture is divided into overlapping subapertures which are processed individually to produce a sequence of images which have coarse resolution in azimuth and fine resolution in range. In the final stage of processing, the coarse-resolution images are coherently combined to produce the final fine-resolution image. In OSA, range and azimuth migration are corrected using complex multiplies; inefficient interpolation operations are not required.

The real-time SAR also incorporates the PGA autofocus algorithm [3] to estimate and remove any residual motion-measurement error that would cause smearing in the azimuth dimension of the image. Autofocus is done in two steps: point selection and phase-error extraction. At the point-select process, the data has only been OSA processed to the coarse-resolution stage in azimuth and fine-resolution in range. The point-select process determines which points (range-azimuth bins) are most suited for extraction of the phase error, and gives the coordinates of these bins to the PGA algorithm. In this manner, autofocus requires less than 1% of the computational load of the image-formation processor.

The PGA algorithm finds the dominant scatterer in each bin and shifts it to zero Doppler frequency in the image domain. The algorithm then assumes any variation from an ideal azimuth-impulse response centered at zero-Doppler is due to residual phase errors. This error is averaged with those errors found from other selected points to yield an estimate for the actual error. The algorithm is iterated until the average detected error level falls below a specified threshold, or until a maximum number of iterations have been performed. The efficiency and robustness of the PGA algorithm is ideally suited for real-time image formation.

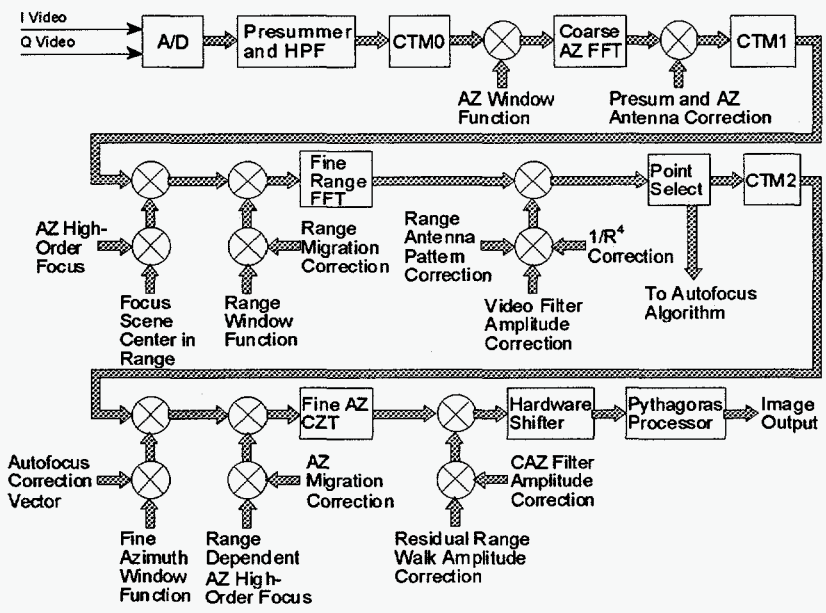


**Figure 7. Functional Diagram of Overlapped Subaperture Algorithm**

## MOTION MEASUREMENT

The SAR motion-measurement and navigation system consists of a miniaturized, high-accuracy, ring-laser-gyro IMU; a 3-axis gimbal antenna-pointing and stabilization assembly; and an autonomous 6-channel P(Y)-code GPS receiver [4]. The system provides four major functions:

- Navigation,
- Motion measurement calculations for SAR motion compensation,
- Antenna pointing and stabilization, and
- Pilot guidance.

The IMU is closely mounted to the antenna to allow measurement of high-frequency motion due to turbulent flight conditions and structural resonances excited by the aircraft engines. The gimbal mounting of the IMU is made possible by its small size and weight. Output from the IMU is fed into the MoComp computer which implements the digital-signal processing and motion calculations of the motion-measurement system. The output of the GPS receiver is also fed into the MoComp computer which implements a nine-error-state Kalman filter to compensate for long-term drift in the IMU measurement. The resulting velocity error of the system is less than 5-cm/sec standard deviation, with an absolute position accuracy of less than 5-m rms for differential-GPS mode. The resulting position and velocity data is fed from the MoComp computer to the radar control and interface computer for SAR motion compensation.

The antenna pointing and stabilization function maintains the boresight of the antenna on either a straight line on the ground (stripmap mode) or a fixed point on the ground (spotlight mode) during each aperture. The pointing accuracy has been measured at less than 0.01-degrees rms. Navigation data from the MoComp computer is provided to the pilots via an aircraft waypoint guidance display (located in the cockpit) which directs the pilot to fly precise trajectories.

## SUMMARY

The Twin-Otter SAR is a state-of-the-art testbed, encompassing four frequency bands and operating over a wide parameter space in resolution and geometry. Exceptional image quality is produced in real-time and in a dynamic flight environment. The testbed is designed to be flexible and can be readily adapted to future experiments. Numerous innovations in real-time hardware and algorithms have been demonstrated and are being transitioned into other programs.

## ACKNOWLEDGMENTS

In addition to the authors of this paper, many individuals at Sandia National Labs were instrumental in the design, development, and support of this system. Sponsors in the development and use of the Twin-Otter SAR testbed include the US Department of Energy, Army, Air Force, Navy, ARPA, Coast Guard, and industry.

## REFERENCES

[1] D. L. Bickel and W. H. Hensley, "Determination of Absolute Interferometric Phase Using the Beam-Amplitude Ratio Technique," 1996 International Geoscience and Remote Sensing Symposium, May 1996.

[2] B. L. Burns and J. T. Cordaro, "A SAR Image-Formation Algorithm that Compensates for the Spatially-Variant Effects of Antenna Motion," SPIE Conference Proceedings, April 1994.

[3] P. H. Eichel, D. C. Ghiglia, and C. V. Jakowatz Jr., "Speckle Processing Method for Synthetic-Aperture-Radar Phase Correction," Optics Letters, Volume 14, Number 1, January 1, 1989.

[4] J. R. Fellerhoff and S. M. Kohler, "Development of a GPS-Aided Motion Measurement, Pointing and Stabilization System for a Synthetic Aperture Radar," Proceedings of the 48th Annual Meeting of The Institute of Navigation, June 1992.